

Analysis of ^{13}C -NMR spectra in C_{60} superconductors: Hyperfine coupling constants, electronic correlation effect, and magnetic penetration depth

N. Sato, H. Tou, and Y. Maniwa*

Department of Physics, Tokyo Metropolitan University, Minami-osawa, Hachi-oji, Tokyo 192-0397, Japan

K. Kikuchi, S. Suzuki, and Y. Achiba

Department of Chemistry, Tokyo Metropolitan University, Minami-osawa, Hachi-oji, Tokyo 192-0397, Japan

M. Kosaka and K. Tanigaki

NEC Corporation, 34 Miyukigaoka, Tsukuba 305, Japan

(Received 19 May 1998; revised manuscript received 6 July 1998)

A ^{13}C -NMR anisotropic hyperfine coupling tensor was determined as $2\pi(-1.68, -1.68, 3.37) \times 10^6$ rad/sec for C_{60}^{3-} in A_3C_{60} superconductors, where A is an alkali metal, by analyzing ^{13}C -NMR spectra below 85 K. Combined with an isotropic coupling constant of $(2\pi \times 0.69) \times 10^6$ rad/sec, the $2s$ and $2p$ characters of the electronic wave functions at the Fermi level were deduced. The results were compatible with local-density-approximation band calculations. From a simulation of ^{13}C -NMR spectra at superconducting state, the traceless chemical (orbital) shift tensor and isotropic chemical shift were determined as (67, 34, -101) ppm and ~ 150 ppm, respectively. An estimated magnetic penetration depth is larger than 570 nm in K_3C_{60} . Furthermore, the modified Korringa relation, $T_1TK^2 \sim \beta S$ (with Knight shift K , spin-lattice relaxation time T_1 , and Korringa constant S), clearly showed the existence of weak but substantial antiferromagnetic spin fluctuation in A_3C_{60} ; $\beta = 0.40$ – 0.58 with an error of $\pm 20\%$. The Stoner enhancement factor was also determined as 1–1.5 from a comparison between spin susceptibility obtained from NMR and band-calculation results. [S0163-1829(98)00542-6]

I. INTRODUCTION

One of the most important quantities to analyze NMR data in metal is a hyperfine coupling constant that describes the interaction between electronic spin and interesting nuclear spin. Although ^{13}C -NMR in C_{60} superconductors A_3C_{60} (where A is alkali metal) has been extensively studied by many authors,^{1–12} a reliable value for this quantity has not yet been determined in this system. For this reason, limited analyses of the NMR data to obtain information on the electronic state have been reported. For example, NMR evidence for the electronic correlation effect in C_{60} superconductors, which has been believed to be important, is still controversial.

However, there are several reports on the hyperfine coupling constants. For example, it was discussed that a dipolar mechanism dominates the ^{13}C spin-lattice relaxation rate $1/T_1$ by Antropov *et al.* on the basis of their band calculations,¹² and by Maniwa *et al.* from the experimental point of view.⁵ A larger isotropic coupling was reported by Kerkoud *et al.*⁶ and Sasaki *et al.*,¹⁰ which corresponds to an isotropic Knight shift of 60–80 ppm in K_3C_{60} at room temperature. An experimental determination of both the isotropic and anisotropic coupling constants, a_{iso} and d , was reported for the first time to our knowledge by Zimmer *et al.* in Rb_3C_{60} .³ Sasaki *et al.* also discussed the ratio in K_3C_{60} .¹⁰ However, it might be difficult to obtain the reliable value in these studies because spin susceptibility of their materials χ_s is almost temperature independent. Recently, this difficulty was overcome by a finding that χ_s of $(\text{NH}_3)\text{K}_3\text{C}_{60}$ shows a

larger temperature dependency.¹³ This and sharp ^{13}C -NMR spectra observed in this material allowed us to determine a_{iso} as $2\pi(0.69 \pm 0.06) \times 10^6$ rad/sec for A_3C_{60} .⁸ The corresponding Knight shift in K_3C_{60} is 37 ppm. However, the d remains to be determined. In this context, we performed a simulation of the ^{13}C -NMR spectra. Using the value for a_{iso} previously reported and the anisotropic Knight shift obtained from the simulation, we successfully determined the value for d in typical C_{60} superconductors K_3C_{60} , Rb_3C_{60} , and $\text{Rb}_2\text{CsC}_{60}$. The results were critically compared with the previous ones and band calculation results.

Based on these studies, we examined the so-called modified Korringa relation, which holds for conventional metals, to study the role of the electronic correlation in A_3C_{60} . Although many authors have suggested the importance of electronic correlation,^{1,14} definite NMR evidence seems not to have been established. Finally, we report an analysis of ^{13}C spectra in the superconducting state of K_3C_{60} that gave information on the chemical (orbital) shift of A_3C_{60} and magnetic penetration depth in the superconducting state.

II. EXPERIMENT AND RESULTS

^{13}C -NMR was observed with conventional pulse and Fourier-transform NMR apparatus at a magnetic field of 4 and 9.4 T. Powder samples of K_3C_{60} and Rb_3C_{60} were prepared by conventional vapor-reaction technique. In K_3C_{60} , ^{13}C was enriched to $\sim 20\%$ from the natural abundance of 1.1%, and the starting C_{60} powder was purified by the sublimation method.¹⁵ Low-field magnetic susceptibility measure-

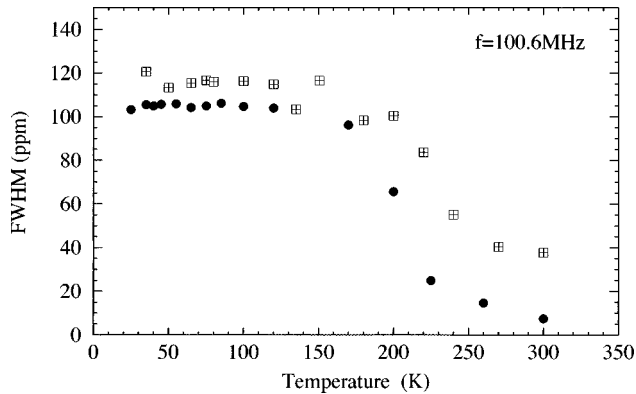


FIG. 1. Temperature dependence of ^{13}C -NMR linewidth [full width at half maximum (FWHM)] in K_3C_{60} and Rb_3C_{60} .

ments gave a superconducting transition temperature T_c of 19 K for K_3C_{60} and 29.5 K for Rb_3C_{60} . The shielding fraction was more than 60% in both the samples.

^{13}C -NMR spectra in K_3C_{60} and Rb_3C_{60} have been known to be strongly temperature dependent at elevated temperatures. In Fig. 1, the full width at half maximum (FWHM) of the ^{13}C -NMR spectra in K_3C_{60} and Rb_3C_{60} is shown. Above ~ 150 K, the linewidth decreases with temperature. Such behavior is interpreted by motional narrowing of the NMR spectra:¹⁶ i.e., above ~ 150 K, C_{60} molecules begin to rotate in a time scale shorter than the inverse of NMR linewidth, ~ 10 μsec . Because this averages out the anisotropy, only the low-temperature spectra ($< \sim 100$ K) were simulated in the present study.

A. Basic assumptions for simulation of ^{13}C -NMR spectra

The NMR frequency shift of a ^{13}C nucleus with gyromagnetic ratio γ_n , Δf is given by the z component of $(\gamma_n/2\pi)\tilde{A}H$, where \tilde{A} is a shielding tensor of second rank and H is an applied magnetic field with components $(0,0,H_0)$.¹⁷ The fractional frequency shift, $\Delta f/f_0$, where f_0 is $\gamma_n H_0/2\pi$, is given by \tilde{A} . In the present paper, Δf is measured from a resonant frequency of TMS (tetramethylsilane), and the positive shift corresponds to a resonance frequency higher than that of TMS at the same field.

There are two types of interactions between electron and interesting nucleus: electronic-spin–nuclear-spin interaction and electronic-orbital–nuclear-spin interaction. We call the shift tensor due to these interactions Knight shift \tilde{K} and chemical shift $\tilde{\sigma}$, respectively. Another important interaction is nuclear-dipole–nuclear-dipole interaction. This is also described by a second-rank tensor. However, it cannot change the isotropic shift or the center-of-mass position in the powder spectrum because this tensor is traceless. In the case of spin larger than one half, there is electronic quadrupole interaction. However, this is not applied to ^{13}C -NMR with spin $\frac{1}{2}$.

In the present simulation, we assumed the following.

(1) An anisotropic (traceless) part of chemical and Knight shift tensors $\tilde{\sigma}$ and \tilde{K} is axial symmetric and its principal axes are the same. Therefore, the principal values for $\tilde{\sigma}$ and \tilde{K} can be denoted by $(\delta_1, \delta_1, \delta_3)$ and (K_1, K_1, K_3) , where $2\delta_1 + \delta_3 = 0$ and $2K_1 + K_3 = 0$, respectively. The total shift

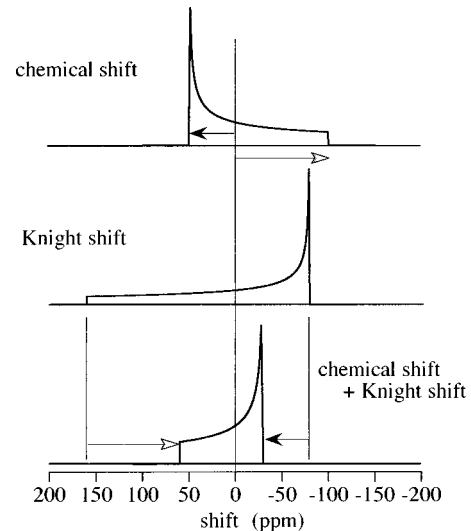


FIG. 2. Powder line shapes: (upper) in the case of axial-symmetric chemical-shift tensor, (middle) in the case of axial-symmetric Knight-shift tensor, and (bottom) in the case of coexistence of axial-symmetric chemical and Knight-shift tensors. Both the chemical and Knight-shift tensors were assumed to be traceless and to have opposite sign from each other: $\delta_1 = \delta_2 > 0$, $K_1 = K_2 < 0$, $2\delta_1 + \delta_3 = 0$, and $2K_1 + K_3 = 0$.

tensor $\tilde{\sigma} + \tilde{K}$ is given by $(\delta_1 + K_1, \delta_1 + K_1, \delta_3 + K_3)$. It is known from a symmetry consideration of the electronic wave function at the carbon site in C_{60} that the third principal axis should be nearly parallel to the carbon $2p_z$ orbital.

(2) Isotropic chemical shift is 150 ppm and temperature independent, as argued in previous reports.⁸ An observed linearity between the ^{13}C shift at room temperature and the square root of the low-temperature ^{13}C spin-lattice relaxation rate, except for ammoniated A_3C_{60} , suggested that the origin of the Knight shift does not significantly change within A_3C_{60} superconductors with face-centered-cubic structure (fcc).^{8,18}

(3) The traceless chemical shift tensor is the same as that of pure C_{60} , and approximated to an axial symmetric tensor with the principal values (54.2, 54.2, -108.4) ppm.^{19,15} Validity of this assumption is given by a simulation of ^{13}C spectra at a superconducting state where the Knight shift disappears, as shown later. It should be also noted that the anisotropic chemical shift of insulating A_6C_{60} is roughly the same as that of pure C_{60} solid: (218, 218, 32) ppm from TMS for K_6C_{60} and (223, 213, 30) ppm from TMS for Rb_6C_{60} with the isotropic shift of 156 ppm.²⁰ This suggests that the chemical shift anisotropy does not significantly vary within A_3C_{60} compounds.

(4) Isotropic Knight shift K_{iso} , is 37 ppm for K_3C_{60} , 41 ppm for Rb_3C_{60} , and 43 ppm for $\text{Rb}_2\text{CsC}_{60}$, which were estimated from the lattice constant at room temperature.⁸ The expected small temperature dependence of a few ppm are ignored. The procedure from (1)–(4) is illustrated in Fig. 2.

(5) There are three carbon sites with intensity ratio of 1:2:2. These carbon sites have different local density of states whose ratio is given by a band calculation; $\sim 4: \sim 7: \sim 12$ for K_3C_{60} , $\sim 3: \sim 4: \sim 7$ for Rb_3C_{60} , and $\sim 3: \sim 4: \sim 7$ for $\text{Rb}_2\text{CsC}_{60}$.²¹ The Knight-shift anisotropy should be proportional to the local density of states. Thus,

the observed line shape is a superposition of three powder line shapes coming from these three carbon sites. However, the site dependence of K_{iso} is ignored, because the absolute value for K_{iso} is much smaller than the Knight-shift anisotropy of 250–300 ppm, as shown later.

(6) Additional inhomogeneity, deviation from axial symmetry, and nuclear-dipolar interaction are included by a convolution of a Gaussian function $\exp[-(\Delta f/\Delta_i)^2]$, where i ($=1,2,3$) denotes the three carbon sites. An inhomogeneity has been actually observed by high-resolution NMR experiments in Rb_3C_{60} even at room temperature where motional narrowing is partially taking place.²⁰ With increasing ^{13}C concentration, homonuclear ^{13}C - ^{13}C dipolar coupling becomes important to the ^{13}C line shape.²² However, the ^{13}C - T_2 measurements indicated that the linewidth due to this coupling is still smaller than ~ 5 ppm at 9.4 T even in the present ^{13}C -enriched sample K_3C_{60} . This value is much smaller than the obtained Gaussian broadening linewidth Δ_i , as well as the anisotropy of Knight-shift and chemical-shift tensors, as shown later.

B. ^{13}C -NMR spectra in normal state

With the above assumptions, we simulated the observed NMR spectra to obtain the traceless Knight-shift tensors ($K_{1,i}, K_{2,i}, K_{3,i}$), where i ($=1,2,3$) denotes the carbon site. The results are shown in Fig. 3. Averaged values for Knight-shift anisotropy $\langle K_3 - K_1 \rangle$ are 252 ppm at 35 K and 259 ppm at 85 K for K_3C_{60} , and 279 ppm at 33 K and 286 ppm at 77 K for Rb_3C_{60} . We also simulated the ^{13}C spectrum of $\text{Rb}_2\text{CsC}_{60}$ reported by Pennington *et al.*⁹ The obtained anisotropy $\langle K_3 - K_1 \rangle = 300$ ppm for $\text{Rb}_2\text{CsC}_{60}$ at 80 K is very close to their estimate of 296 ppm in which only a single traceless Knight-shift tensor was considered. Similarly, a traceless Knight-shift tensor (216, -92 , -124) ppm determined by Zimmer *et al.* for Rb_3C_{60} at room temperature (RT), based on the assumption of single traceless Knight-shift tensor,³ is close to the present result (190.7, -95.3 , -95.3) ppm. These agreements suggest that the averaged Knight-shift anisotropy can be obtained within $\sim 15\%$ accuracy, irrespective of a single or a three Knight-shift tensor assumption.

To obtain good fitting, however, we need the large inhomogeneity of $\Delta_i = 40\text{--}60$ ppm. Although this is partially due to a deviation from axial-symmetric chemical and Knight-shift tensors, there must be a large distribution of carbon atoms with different electronic states.

The ratio of a traceless Knight shift to an isotropic one $\langle K_3 - K_1 \rangle / K_{\text{iso}}$ is 7.27 (7.46) at 33 (85) K for K_3C_{60} , 7.17 (7.34) at 33 (77) K for Rb_3C_{60} , and 7.35 at 80 K for $\text{Rb}_2\text{CsC}_{60}$. These values are very close to each other, suggesting that the electronic wave functions at the Fermi level have essentially the same characteristics in these fcc A_3C_{60} compounds as discussed later. An average value of 7.32 is in good agreement with 6.9 ($=324$ ppm/47 ppm) estimated from the Knight shift reported by Zimmer *et al.* for Rb_3C_{60} .³ However, it is quite different from 3.85 ($=3/0.78$) by Sasaki *et al.*¹⁰ We believe that in their fitting and data quality it is difficult to deduce a usefully accurate Knight-shift tensor from the ^{13}C -NMR spectra with linewidth much larger than the expected isotropic shift.

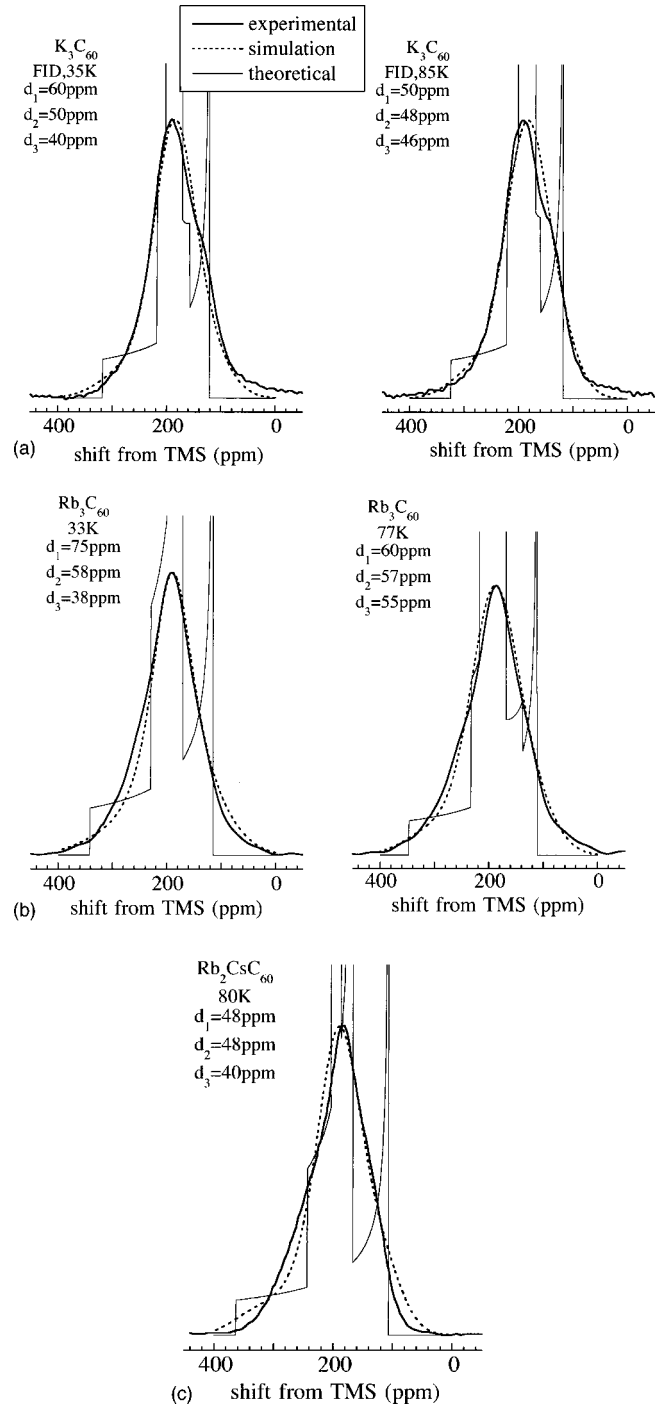


FIG. 3. Comparison of experimentally observed ^{13}C -NMR spectra with simulated line shapes: (a) for K_3C_{60} , (b) for Rb_3C_{60} , and (c) for $\text{Rb}_2\text{CsC}_{60}$. The spectrum of (c) was taken from Ref. 9.

From the above estimate of $\langle K_3 - K_1 \rangle / K_{\text{iso}}$ and the value for a_{iso} , we can obtain the anisotropic (traceless) hyperfine coupling tensor (d_{11}, d_{11}, d_{33}) as $d_{11} = -d_{33}/2 = -2.44a_{\text{iso}} = -2\pi \times 1.68(10^6 \text{ rad/sec})$ per C_{60}^{3-} . Here, d_{11} , d_{33} , and a_{iso} are defined by

$$K_i = \frac{d_{ii}}{\hbar \gamma_e \gamma_n} \chi_s \quad (i=1,2,3), \quad K_{\text{iso}} = \frac{a_{\text{iso}}}{\hbar \gamma_e \gamma_n} \chi_s, \quad (1)$$

where χ_s is the spin susceptibility per C_{60} , and γ_e (γ_n) > 0 is the electronic (^{13}C -nuclear) gyromagnetic ratio. Further, we have

$$\chi_s = 2\alpha\mu_B^2 N(E_F) = \frac{1}{2}\alpha(\hbar\gamma_e)^2 N(E_F), \quad (2)$$

where $N(E_F)$ is electronic density of states at the Fermi level for one spin direction and $\alpha = 1/[1 - IN(E_F)]$ an enhancement factor, the so-called Stoner factor, and μ_B is the Bohr magneton.

On the other hand, the anisotropic (axial-symmetric) Knight shift, which is due to dipolar interaction with electronic spins in the carbon $2p_z$ orbital, is given by

$$K_1 = K_2 = -\frac{K_3}{2} = -\frac{2}{5} \left\langle \frac{1}{r^3} \right\rangle_{E_F} \chi_s. \quad (3)$$

Therefore, d_{11} ($= -d_{33}/2$) is $-0.4\langle 1/r^3 \rangle_{E_F} (\hbar\gamma_e\gamma_n)$ due to the dipolar interaction, where $\langle \rangle_{E_F}$ means an average of the distance between electronic spin and the interesting nuclear spin over the conduction electron wave function $u(r)$ normalized in the C_{60} unit at the Fermi level.^{23,5} The obtained values for (d_{11}, d_{11}, d_{33}) lead to $\langle 1/r^3 \rangle = 0.0315a_B^{-3}$, where a_B is the Bohr radius. If we normalize the wave function in the carbon atom, we have $\langle 1/r^3 \rangle = 60 \times 0.0315 = 1.89a_B^{-3}$. This is very close to a value of $\langle 1/r^3 \rangle = 1.7a_B^{-3}$ for the $2p_z$ orbital of a free carbon atom, suggesting that the wave function at the Fermi level mainly consists of the carbon $2p_z$ orbital. [Here, we considered that the wave function is a linear combination of the carbon $2p_z$ and $2s$ orbitals as $u(r) = a\phi_{2p_z} + b\phi_{2s}$ with $a^2 + b^2 = 1$.] However, this value is substantially smaller than $3.71a_B^{-3}$ obtained for K_3C_{60} using an *ab initio* local-density-approximation calculation by Antropov *et al.*¹² Such a large value was explained by a compression of the wave function in the crystal. One possibility for the difference is a mixing of $2p_x$ and $2p_y$ orbitals to the wave function, which was neglected in the present analysis. If we include $2p_x$ and $2p_y$ components, the right-hand side of Eq. (3) should be multiplied by a factor smaller than unity, and thus we would have a larger value for $\langle 1/r^3 \rangle$.

Similarly, we can estimate a carbon $2s$ component in the conduction-electron wave function using a_{iso} given by $(8\pi/3)\langle |u(0)|^2 \rangle (\hbar\gamma_e\gamma_n)$. We obtain $\langle |u(0)|^2 \rangle = 0.037a_B^{-3}$ for the wave function normalized in carbon atom. This value is compared with $2.767a_B^{-3}$ for the free-carbon $2s$ orbital. The ratio of these values gives a measure of the $2s$ component in the conduction-electron wave function at E_F : $\sim 1.3\%$. The result is in fairly good agreement with those of calculations using the full-potential linear muffin-tin orbital (LMTO) method: $N_s(E_F)/N_p(E_F)$ of 1.3–4.2% depending on the three carbon sites for K_3C_{60} .²¹ Here $N_s(E_F)$ and $N_p(E_F)$ are the density of states at the Fermi level from carbon $2s$ and $2p_z$ orbitals, respectively. The present result is also consistent with a previous estimate by ^{13}C -NMR: $N_s(E_F)/N_p(E_F) < 1/45$.⁵ However, an estimated value of $\sim 1/150$ by Antropov *et al.* seems to be slightly smaller than the present result.¹² It is also compared with a high-resolution solution NMR study that led to the 3% s character ‘‘left’’ in the p_z orbital.²⁴

The hyperfine coupling constant should be also estimated from an EPR experiment.²⁵ However, in the present case, there is no report for the C_{60}^{3-} ion within our knowledge.¹⁴ Therefore, the present study is the first complete determination of ^{13}C hyperfine coupling constants for C_{60}^{3-} .

C. Korringa relation and electronic correlation

Next, we discuss the modified Korringa relation. In the case of the isotropic hyperfine interaction,²⁶ the Korringa relation is given by

$$(T_1 T)_{\text{iso}} K_{\text{iso}}^2 = \beta S, \quad (4a)$$

$$S = \left(\frac{\gamma_e}{\gamma_n} \right)^2 \left(\frac{\hbar}{4\pi k_B} \right), \quad (4b)$$

where deviation of β from unity is a sign of the importance of electron-electron interaction (electronic correlation), and the Korringa constant S is 4.165×10^{-6} (sec K) for ^{13}C nucleus. For the dipolar interaction (dipolar mechanisms),^{5,23} the powder (angular) averaged T_1 is related to Knight shift as

$$\left\langle \frac{1}{T_1 T} \right\rangle_{\text{dip}} = \left(\frac{\pi}{2} \right) k_B \hbar^3 (\gamma_n \gamma_e)^2 \left[\frac{4}{5} \left\langle \frac{1}{r^3} \right\rangle N(E_F) \right]^2 = \left(\frac{2}{S} \right) K^2, \quad (5)$$

where we neglected the effect of electronic correlation.

If there are the above two types of interaction,²³ $\langle 1/T_1 T \rangle$, after averaged over the three carbon sites, is expressed as

$$\left\langle \frac{1}{T_1 T} \right\rangle = \left\langle \frac{1}{T_1 T} \right\rangle_{\text{dip}} + \left(\frac{1}{T_1 T} \right)_{\text{iso}} = \left(\frac{1}{\beta S} \right) (2\langle K_1^2 \rangle + \langle K_{\text{iso}}^2 \rangle). \quad (6)$$

In this formula, an enhancement factor β was introduced as in Eq. (4a), and $\langle K^2 \rangle$ means the site average. A similar formula for a single shift tensor has also been deduced by Mehring *et al.*²⁷

Using the site-averaged values for $\langle 1/T_1 T \rangle$ and $\langle K_1^2 \rangle$, we obtain the enhancement factor β as shown in Table I. The reliability in this estimate of the absolute value for β may be $\pm 20\%$, which is partially due to the definition of T_1 ($\sim 10\%$) and the other comes from Knight-shift determination ($\sim 10\%$). Therefore, β is $(0.40 \pm 0.08) - (0.58 \pm 0.17)$ and temperature independent as is usual for a Fermi liquid in the temperature range studied. It shows that the deviation from Korringa relation for noninteracting electrons, that is, the deviation from unity in β is not so large compared with conventional metals with $\beta \sim 1$. However, β is smaller than unity. This means that the enhancement of $1/T_1$ due to anti-ferromagnetic spin fluctuation is more significant than ferromagnetic enhancement in K . [K is proportional to dynamic spin susceptibility with $q=0$ and $\omega=0$, $\chi(0,0)$, while $1/T_1$ is proportional to the q sum of $\chi(q,\omega)$.]

The present results for β are compared with those obtained by Mehring *et al.* 1/2.5 for Rb_3C_{60} and 1/2.7 for K_3C_{60} at 300 K.²⁷ Although their estimated hyperfine coupling constants are ~ 3 times larger than the present values, the obtained β is very close to each other. This is because Eq. (6) does not explicitly include the values for the coupling constants.

The electronic correlation in A_3C_{60} has also been discussed by Pennington *et al.* in terms of Korringa relation.⁹ Based on a measurement of frequency (shift)-dependent T_1 in the observed spectra and on an assumption of single Knight-shift tensor, they considered that the dipolar contribution to $1/T_1$, $(1/T_1)_{\text{dip}}$, would be about half of the $1/T_1$

TABLE I. Parameters obtained from the simulation of ^{13}C -NMR spectra, superconducting transition temperature T_c , and ^{13}C spin-lattice relaxation time T_1 deduced from the three-component fit of relaxation curves (Ref. 5) that is slightly shorter than stretched exponential value. The spectrum of $\text{Rb}_2\text{CsC}_{60}$ was taken from Ref. 9. The values for β previously reported are also shown for a comparison. β is defined by $T_1 T K^2 \sim \beta S$.

Sample	$[\langle(K_3 - K_1)^2\rangle]^{0.5}$ (ppm)	K_{iso} (ppm)	$\langle 1/T_1 T \rangle$ (1/sec/K)	T_c (K)	β
K_3C_{60} at 30 K	269	37	1/137	19	0.58
85 K	276	37	1/132	19	0.58
Rb_3C_{60} at 33 K	294	41	1/96	29	0.48
77 K	301	41	1/91	29	0.48
$\text{Rb}_2\text{CsC}_{60}$ at 80 K	316	43	1/69	31	0.40
K_3C_{60} at 300 K (Ref. 27)					1/2.5
Rb_3C_{60} at 300 K (Ref. 27)					1/2.7
K_3C_{60} (Ref. 5)					0.4–1.8
$\text{Rb}_2\text{CsC}_{60}$ at 80 K (Ref. 9)					
			(Null evidence for strong correlation)		
K_3C_{60} below 300 K (Ref. 10)					1/(7.4±0.1)

observed. From the obtained $(1/T_1)_{\text{dip}}$ and Korringa relation with $\beta \sim 1$, they successfully reproduced the observed line shape. Thus, they suggested null evidence for strong correlation in A_3C_{60} superconductors. However, it is not clear that the observed frequency dependence in T_1 is directly related to T_1 anisotropy in the case of the presence of different (or a large number of different) carbon sites with different electronic density of states. Maniwa *et al.* also discussed Korringa relation in A_3C_{60} .⁵ Their analysis gives only a range of 0.4–1.8 for β . On the other hand, Sasaki *et al.* reported a substantially larger enhancement factor: $K(\alpha) \equiv 1/\beta = 7.4 \pm 0.1$.¹¹ Their argument is based on the value of $a_{\text{iso}}/d_{11} = -0.78$ for the ratio of the hyperfine coupling constant, which is much larger than the present result, and also based on deduction of $(1/T_1)_{\text{iso}}$ from the observed $(1/T_1)_{\text{obs}}$. It is apparently known that $(1/T_1)_{\text{iso}}$ is much smaller than $(1/T_1)_{\text{obs}}$ at low temperatures. However, they considered that $(1/T_1)_{\text{iso}}$ becomes equal to $(1/T_1)_{\text{obs}}$ at high temperatures because the anisotropic hyperfine coupling could be averaged out by C_{60} molecular rotation. This is unlikely to occur. Even at high temperatures where C_{60} exhibits a large-amplitude molecular rotation, the observed $(1/T_1)$ should be just a site- and angular-averaged value. This does not mean that the contribution from the dipolar interaction to $(1/T_1)$ can be ignored.

D. Stoner enhancement

The electronic density of states at the Fermi level $N(E_F)$ can be also discussed. Using Eqs. (1), (2), and (6), we have

$$\left\langle \frac{1}{T_1 T} \right\rangle = \left(\frac{\alpha^2}{\beta} \right) (\pi k_B \hbar) (2d_{11}^2 + a_{\text{iso}}^2) N(E_F)^2. \quad (7)$$

Substitution of the values for d_{11} and a_{iso} into Eq. (7) leads to

$$N(E_F) = 152 \left(\frac{\sqrt{\beta}}{\alpha} \right) \sqrt{\left\langle \frac{1}{T_1 T} \right\rangle} \quad (\text{states/eV spin } \text{C}_{60}). \quad (8)$$

For K_3C_{60} with $\beta = 0.58$ and $\langle 1/T_1 T \rangle \sim 1/137$ (1/sec K), $N(E_F) = 9.9, 6.6,$ and 4.9 (states/eV spin C_{60}) for $\alpha = 1, 1.5,$ and 2.0 , respectively. It is difficult to estimate α from experimental data alone. Here, we employ the values of band-structure calculations,^{12,21,28–30} which give around 9 states/eV spin C_{60} for K_3C_{60} for an orientationally ordered state, as shown in Table II.

One example of $N(E_F)$ as a function of the lattice constant, calculated by Huang *et al.*³⁰ is shown in Fig. 4, along with $\alpha N(E_F) = \chi_s/2\mu_B^2$ obtained from a NMR Knight shift at RT.⁸ The difference in Fig. 4 indicates that α is ~ 1.14 . Unexpectedly, it seems to be independent of the lattice constant. This may be an anomaly in materials close to the insulating phase that would appear with increasing lattice constant.

However, the real systems have C_{60} merohedral disorder, which substantially changes the structures of the density of states.³¹ Recently, it was reported that $N(E_F)$ of the disordered system is reduced by 15–20% (Ref. 32) or increased by $\sim 20\%$ (Ref. 33) compared to that of the ordered system. In the experimental point of view, it is difficult to determine whether the disorder leads to an increase or decrease in $N(E_F)$, although the spin susceptibility of $\text{Na}_2\text{AC}_{60}$ has been found to be slightly larger in the orientationally disordered phase than the ordered simple-cubic phase at low temperature.³⁴ Therefore, we just note that α is not so large, probably in a range of 1 to 1.5, taking the reduction factor of $\pm 20\%$ into account.

TABLE II. The density of states at the Fermi level $N(E_F)$ (per eV and spin) for K_3C_{60} obtained by local-density-approximation calculations.

Reference	$N(E_F)$ states/eV spin C_{60}
28	6.1
29	12.5
30	8.98
21	9.34
12	9.0
Average	9.18

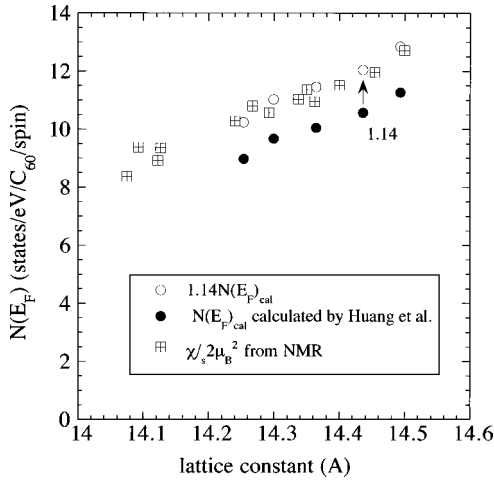


FIG. 4. The density of states at the Fermi level as a function of the lattice constant. Squares were obtained from NMR Knight-shift measurement (Ref. 8). The origin of the Knight shift is assumed to be 148.5 ppm. Closed circles are band-calculation results by Huang *et al.* (Ref. 30).

E. ^{13}C -NMR spectra in superconducting state

NMR frequency shift in superconducting state is given by

$$\delta = \delta_{\text{orb}} + K + \delta_{\text{dia}}. \quad (9)$$

Here, δ_{orb} is an orbital shift (or chemical shift) and usually temperature independent even at the superconducting state. On the other hand, Knight shift K decreases with temperature, and follows a Yoshida function.³⁵ Such behavior was actually observed by Stenger *et al.*³⁶ which indicated that isotropic Knight shifts of alkali-metal NMR of A_3C_{60} superconductors are described as typical weak-coupling superconductors with $K \sim 0$ at $T \sim 0$. The third term of Eq. (9) is a diamagnetic field due to superconducting shielding. When the vortex forms a triangular lattice,³⁷ it is given by

$$\delta_{\text{dia}} = \frac{(1-N)}{H} \frac{\Phi_0}{4\pi\lambda^2} \ln\left(0.381e^{-0.5} \frac{d}{\xi}\right), \quad (10)$$

where Φ_0 is flux quantum, λ magnetic penetration depth, d the nearest-neighbor vortex distance, ξ coherence length, and N the demagnetization factor. Using these equations together with Eq. (11), we can obtain isotropic and anisotropic chemical shift and the penetration depth λ .

Figure 5 shows the temperature dependence of ^{13}C -NMR spectra in K_3C_{60} observed at 9.4 T. Significant change of the line shape can be observed. The isotropic shift δ_{iso} and the linewidth (FWHM) $\Delta\delta$ are shown in Fig. 6. An rf frequency-shift measurement indicated that the superconducting transition temperature is around 15.5 K at 9.4 T. Roughly speaking, the high-field shift with decreasing temperature, which corresponds to the decrease of the spin susceptibility, suggests formation of spin-singlet Cooper pairs. The line broadening should be ascribed to the field inhomogeneity caused by formation of a vortex lattice.

Assuming that the isotropic and anisotropic Knight shifts are zero at the lowest temperature 4.2 K, we simulated the line shape at 4.2 K. In this simulation, we assumed that all the carbons have the same nonaxial chemical-shift tensor, as used in the previous analysis of pure C_{60} solid.^{15,19} The as-

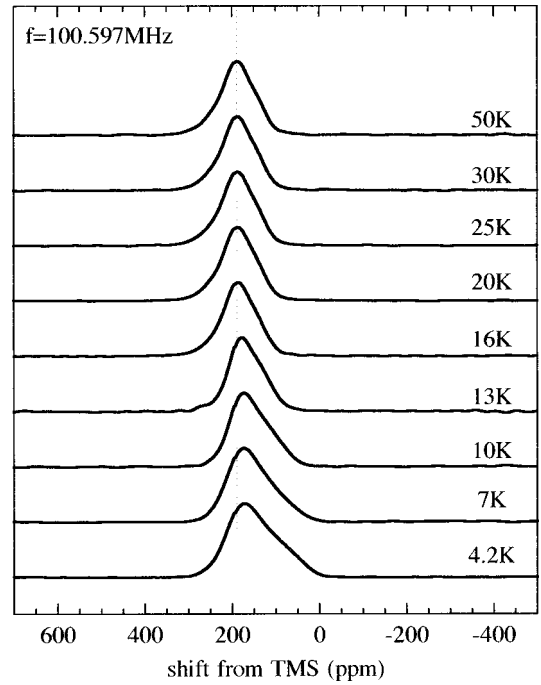


FIG. 5. Temperature dependence of ^{13}C -NMR spectra in K_3C_{60} measured at 9.4 T.

sumption is based on an observation that almost all the sp^2 carbons give a similar or typical chemical-shift line shape.¹⁷ The result is shown in Fig. 7. Parameters obtained are (215, 182, 47) ppm from TMS for the chemical-shift tensor, and the convolution function is $\exp(-\delta^2/\Delta^2)$ with $\Delta = 43$ ppm. This means that the anisotropy of the chemical shift is (67, 34, -101) ppm and the isotropic shift is 148 ppm. These are compared with (70, 39, -110) ppm and 143 ppm for pristine

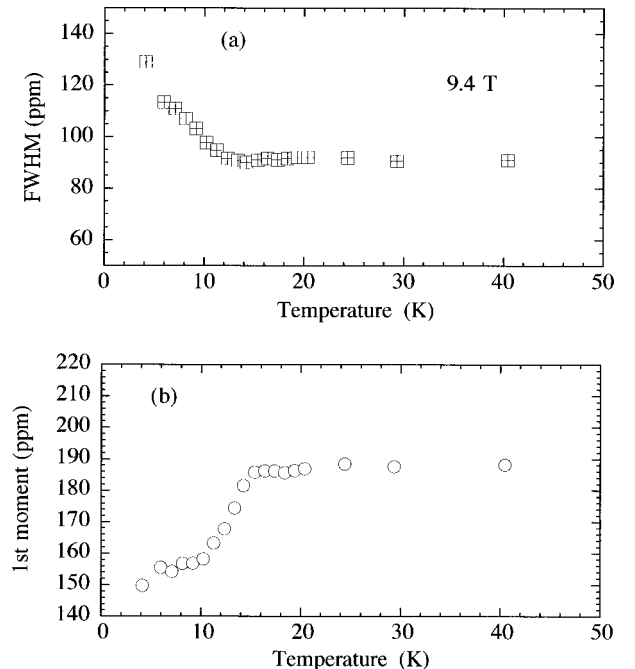


FIG. 6. Temperature dependences of (a) the linewidth and (b) center-of-mass position of ^{13}C -NMR spectra in K_3C_{60} measured at 9.4 T.

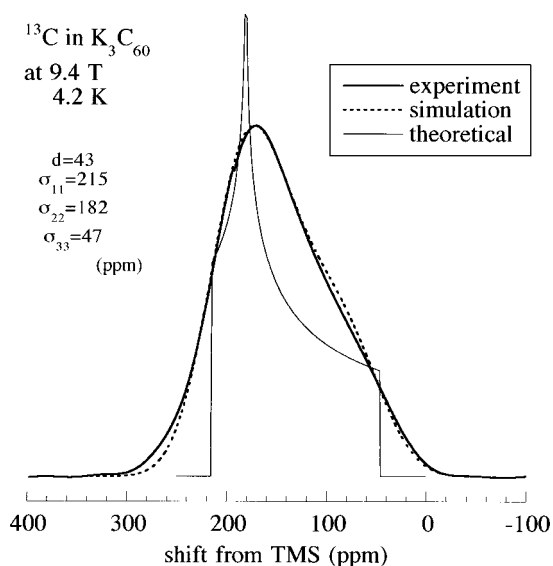


FIG. 7. Comparison of experimentally observed ^{13}C -NMR spectrum with simulated line shape at 4.2 K in the superconducting state. In the simulation, single chemical-shift tensor (215, 182, 47) ppm was assumed and Gaussian convolution of a width of 43 ppm was used to take an additional broadening into account.

C_{60} solid.¹⁹ It is found that the anisotropy is very close to that of pristine C_{60} , supporting assumption (3) in Sec. II A.

Next we discuss the additional broadening of $\Delta = 43$ ppm ($=4.0$ G). In the vortex state, the second moment of the field inhomogeneity due to vortex lattice ΔH^2 is approximated to³⁸

$$\sqrt{\Delta H^2} = \frac{\Phi_0}{\lambda^2 \sqrt{16\pi^3}}. \quad (11)$$

The observed second moment is $\Delta^2/2 = 8.0 \text{ G}^2 = (2.83 \text{ G})^2$ for the Gaussian line shape. Using this value, we have 570 nm for λ from Eq. (11). This value is compared to 600 nm obtained from NMR (Ref. 2) and 480 nm obtained from muon spin relaxation.³⁹ Furthermore, if we use 3 nm for ξ (Ref. 40)

and $N = 1/3$, $\delta_{\text{dia}} = 7.2$ ppm. In this case, the isotropic chemical shift is $148 + 7.2 \sim 155.2$ ppm, slightly larger than 150 ppm used in the simulation of normal states. This value for λ is, however, a lower limit, because there would be an additional broadening, for example, caused by inhomogeneity of δ_{dia} in the crystal. Then, we estimate in an alternative way as follows. The value for λ recently determined by magnetic susceptibility measurements for K_3C_{60} single crystals is ~ 853 nm on average, which distributes in a range of 770–1020 nm.⁴⁰ This value leads to $\delta_{\text{dia}} = 3.2$ ppm and $\delta_{\text{iso}} = 151$ ppm, supporting assumptions (2) and (3).

III. SUMMARY

In summary, we determined the anisotropic hyperfine coupling tensor as $2\pi(-1.68, -1.68, 3.37)$ (10^6 rad/sec) for C_{60}^{3-} . Combined with the isotropic hyperfine coupling constant of $a_{\text{iso}}/2\pi = (0.69 \pm 0.06) \times 10^6$ rad/sec, the present results indicate that the conduction-electron wave functions at the Fermi level mainly consist of a carbon $2p_z$ orbital. The result roughly agrees with band calculations, while the contribution from the $2s$ state to ^{13}C - $1/T_1$ is slightly larger than the estimate of Antropov *et al.* based on local-density-approximation calculation. The Korringa relation examined provided evidence for the existence of weak but substantial antiferromagnetic fluctuation in A_3C_{60} . This should be ascribed to an electronic correlation effect or the combined effect of a short mean free path with electronic correlation in the materials.⁴¹ An analysis of the ^{13}C -NMR spectrum of the superconducting state justified the assumptions used in the simulation at normal state and the origin of the Knight shift.⁸

ACKNOWLEDGMENTS

We thank T. Kodama and T. Kato for useful discussions. This work was supported in part by a grant-in-aid from the Ministry of Education, Science and Culture and by the fund for Special Research Projects at Tokyo Metropolitan University.

*Author to whom all correspondence should be addressed. Electronic address: maniwa@phys.metro-u.ac.jp

¹For a review, C. H. Pennington and V. A. Stenger, *Rev. Mod. Phys.* **68**, 855 (1996).

²R. Tycko, G. Dabbagh, M. J. Rosseinsky, D. W. Murphy, A. P. Ramirez, and R. M. Fleming, *Phys. Rev. Lett.* **68**, 1912 (1992).

³G. Zimmer *et al.*, *Europhys. Lett.* **24**, 59 (1993).

⁴G. Quirion, C. Bourbonnais, E. Barthel, P. Auban, D. Jerome, J. M. Lambert, A. Zahab, P. Bernier, C. Febre, and A. Rassat, *Europhys. Lett.* **21**, 233 (1993).

⁵Y. Maniwa *et al.*, *J. Phys. Soc. Jpn.* **63**, 1139 (1994).

⁶R. Kerkoud *et al.*, *Europhys. Lett.* **25**, 379 (1994).

⁷Y. Maniwa *et al.*, *Phys. Rev. B* **52**, R7054 (1995).

⁸Y. Maniwa *et al.*, *Phys. Rev. B* **54**, R6861 (1996).

⁹C. H. Pennington *et al.*, *Phys. Rev. B* **53**, R2967 (1996).

¹⁰S. Sasaki *et al.*, *Physica C* **278**, 223 (1997).

¹¹S. Sasaki *et al.*, *Physica C* **278**, 238 (1997).

¹²V. P. Antropov, I. I. Mazin, O. K. Andersen, A. I. Liechtenstein, and O. Jepsen, *Phys. Rev. B* **47**, 12 373 (1993).

¹³Y. Iwasa *et al.*, *Phys. Rev. B* **53**, R8836 (1996).

¹⁴For a review, M. S. Dresselhaus, G. Dresselhaus, and P. Eklund, *Science of Fullerenes and Carbon Nanotubes* (Academic, San Diego, 1996).

¹⁵Y. Maniwa *et al.*, *Jpn. J. Appl. Phys., Part 2* **33**, L173 (1994).

¹⁶R. Tycko *et al.*, *Science* **253**, 884 (1991).

¹⁷For example, M. Mehering, *High Resolution NMR Spectroscopy in Solids* (Springer-Verlag, New York, 1991).

¹⁸Y. Maniwa *et al.*, in *Electrochemical Society Proceedings*, edited by K. M. Kadish and R. S. Ruoff (Electrochemical Society, New York, 1997), Vol. 97-14, p. 1191.

¹⁹R. Tycko *et al.*, *Phys. Rev. Lett.* **67**, 1886 (1991).

²⁰J. Reichenbach *et al.*, *J. Chem. Phys.* **101**, 4585 (1994).

²¹D. L. Novikov, V. A. Gubanov, and A. J. Freeman, *Physica C* **191**, 399 (1992).

²²K. Eichele and R. E. Wasylshen, *J. Comput. Chem.* **98**, 3108 (1994).

²³Y. Maniwa, K. Kume, H. Suematsu, and S. Tanuma, *J. Phys. Soc. Jpn.* **54**, 666 (1985).

- ²⁴J. M. Hawkins *et al.*, *J. Am. Chem. Soc.* **113**, 7770 (1991).
- ²⁵For a review, see J. R. Morton, *Chem. Rev.* **64**, 453 (1964).
- ²⁶For example, C. P. Slichter, *Principles of Magnetic Resonance* (Springer-Verlag, New York, 1990).
- ²⁷M. Mehring *et al.*, *Philos. Mag. B* **70**, 787 (1994).
- ²⁸S. C. Erwin and W. E. Pickett, *Science* **254**, 842 (1991).
- ²⁹S. Saito and A. Oshiyama, *Solid State Commun.* **82**, 41 (1992).
- ³⁰M. Z. Huang *et al.*, *Phys. Rev. B* **46**, 6572 (1992).
- ³¹M. P. Gelfand and J. P. Lu, *Phys. Rev. Lett.* **68**, 1050 (1992).
- ³²F. Aryasetiawan *et al.*, *Phys. Rev. B* **55**, R10 165 (1997).
- ³³J. Lu and L. Zhang, *Solid State Commun.* **105**, 99 (1997).
- ³⁴T. Saito *et al.*, *J. Phys. Soc. Jpn.* **64**, 4513 (1995).
- ³⁵K. Yoshida, *Phys. Rev.* **110**, 769 (1958).
- ³⁶V. A. Stenger *et al.*, *Phys. Rev. B* **48**, 9942 (1993).
- ³⁷P. G. Gennes, *Superconductivity of Metals and Alloys* (Benjamin, New York, 1966).
- ³⁸P. Pincus *et al.*, *Phys. Lett.* **13**, 21 (1964).
- ³⁹Y. J. Uemura *et al.*, *Nature (London)* **352**, 605 (1991).
- ⁴⁰V. Buntar *et al.*, *Phys. Rev. B* **56**, 14 128 (1997).
- ⁴¹B. S. Shastry and E. Abrahams, *Phys. Rev. Lett.* **72**, 1933 (1994).